ARL-TN-1162 ● JUNE 2023

Condensed-Phase Property Estimates for 1,5,9-Decatriene and Myrcene Derived from Atomistic Molecular Dynamics Simulations

by Jeffrey D Veals, Chiung-Chu Chen, In-Chul Yeh, Christopher P Stone, and Michael J McQuaid

NOTICES

Disclaimers

The findings in this report are not to be construed as an official Department of the Army position unless so designated by other authorized documents.

Citation of manufacturer's or trade names does not constitute an official endorsement or approval of the use thereof.

Destroy this report when it is no longer needed. Do not return it to the originator.

ARL-TN-1162 ● JUNE 2023

Condensed-Phase Property Estimates for 1,5,9-Decatriene and Myrcene Derived from Atomistic Molecular Dynamics Simulations

Jeffrey D Veals, Chiung-Chu Chen, In-Chul Yeh, Christopher P Stone, and Michael J McQuaid
DEVCOM Army Research Laboratory

REPORT DOCUMENTATION PAGE

1. REPORT DATE	2. REPORT TYPE	3. DATES COVERED	
		START DATE	END DATE
June 2023	Technical Note	11/01/2022	4/26/2023

4. TITLE AND SUBTITLE
Condensed-Phase Property Estimates for 1,5,9-Decatriene and Myrcene Derived from Atomistic Molecular Dynamics Simulations

5a. CONTRACT NUMBER	5b. GRANT NUMBER	5c. PROGRAM ELEMENT NUMBER
5d. PROJECT NUMBER	**5e. TASK NUMBER**	**5f. WORK UNIT NUMBER**

6. AUTHOR(S)
Jeffrey D Veals, Chiung-Chu Chen, In-Chul Yeh, Christopher P Stone, and Michael J McQuaid

7. PERFORMING ORGANIZATION NAME(S) AND ADDRESS(ES)	8. PERFORMING ORGANIZATION REPORT NUMBER
DEVCOM Army Research Laboratory ATTN: FCDD-RLA-WC Aberdeen Proving Ground, MD 21005	ARL-TN-1162

9. SPONSORING/MONITORING AGENCY NAME(S) AND ADDRESS(ES)	10. SPONSOR/MONITOR'S ACRONYM(S)	11. SPONSOR/MONITOR'S REPORT NUMBER(S)

12. DISTRIBUTION/AVAILABILITY STATEMENT
Approved for public release: distribution unlimited.

13. SUPPLEMENTARY NOTES
ORCID IDs: Jeffrey D Veals, 0000-0002-8238-345X; Chiung-Chu Chen, 0000-0002-8666-9949; Christopher P Stone, 0000-0002-9621-5334; Michael J McQuaid; 0000-0001-5523-7468

14. ABSTRACT
In support of a program to develop and apply machine learning methods to accelerate the creation of detailed finite-rate chemical kinetics mechanisms, atomistic molecular dynamics methods were employed to obtain estimates for some condensed-phase properties of 1,5,9-decatriene and myrcene. Protocols for estimating their densities, enthalpies of vaporization, and self-diffusion coefficients as a function of temperature are summarized and the results presented. The enthalpy-of-vaporization estimates were combined with gas-phase enthalpy-of-formation estimates to obtain condensed-phase enthalpy-of-formation estimates for the pair. The self-diffusion coefficient estimates were employed to parameterize a function we use in computing rate coefficients for elementary condensed-phase reactions. Those results are also presented and discussed.

15. SUBJECT TERMS
Weapons Sciences, propulsion, chemical kinetics, machine learning, free volume theory

16. SECURITY CLASSIFICATION OF:			17. LIMITATION OF ABSTRACT	18. NUMBER OF PAGES
a. REPORT	b. ABSTRACT	c. THIS PAGE		
Unclassified	Unclassified	Unclassified	UU	31

19a. NAME OF RESPONSIBLE PERSON	19b. PHONE NUMBER *(Include area code)*
Michael J McQuaid	(410) 278-6185

STANDARD FORM 298 (REV. 5/2020)
Prescribed by ANSI Std. Z39.18

Contents

List of Figures

List of Tables

Acknowledgments

Funding for this study was provided by the US Army Combat Capabilities Development Command Army Research Laboratory's Machine Learning to Accelerate Detailed Finite-Rate Chemical Kinetics Mechanism Creation for Continuum-Level Modeling of Energetic Material Decomposition and Combustion mission program. The molecular dynamics simulations were performed on DoD High Performance Computing Modernization Program computing platforms.

1. Introduction

Under a US Army Combat Capabilities Development Command Army Research Laboratory mission program, machine learning (ML) methods with the potential to accelerate the creation of detailed finite-rate chemical kinetics mechanisms for modeling the decomposition and combustion of energetic materials (EMs) are being developed and evaluated. The framework for the effort predicates employing results produced by canonical thermochemical kinetics models to train neural networks (NNs) to rank the relative importance of elementary chemical reactions that an enumerator generates for specific applications. Among the bases for the effort will be a comprehensive detailed gas-phase finite-rate chemical kinetics mechanism for representing the pyrolysis and combustion of 1,5,9-decatriene (DTE) and myrcene (MYR). Currently under development (Chen et al. 2023), the mechanism for these $C_{10}H_{16}$ isomers will serve two purposes. The first is as a standard with which to evaluate the reliability of ML-based reaction ranking algorithms trained on modeling results produced for smaller hydrocarbons such as 1,3-butadiene (C_4H_6). The second is as a template for a reaction enumerator that will be employed to generate candidate reactions for modeling the decomposition and combustion of larger hydrocarbons such as 6-ethenyl-2,8,12,16-octadecetetraene (EODT, $C_{20}H_{32}$).

The selection of a mechanism for modeling the pyrolysis and combustion of DTE and MYR for these purposes was based on several considerations. Since 2008, we have been developing and applying a detailed mechanism for modeling the pyrolysis and combustion of EODT. Motivated by the premise that in deflagration scenarios EODT would be more representative of the nascent products of hydroxyl-terminated polybutadiene-type R45M's pyrolysis than a relatively light hydrocarbon such as 1,3-butadiene, the mechanism constructed to model EODT's combustion now comprises more than 5400 reactions and 1300 species. However, to the extent EODT is merely representative of the nascent products of R45M's pyrolysis in deflagration scenarios and (to our knowledge) is not commercially available, we assumed that our capacity to find and/or produce measurement-based data that could be employed to establish (without significant caveats) the validity and comprehensiveness of the EODT mechanism would be extremely limited.

To address that issue, we sought to establish as a benchmark a mechanism for a relatively inexpensive, commercially available hydrocarbon with a well-defined molecular structure having from 8 to 20 carbon atoms that, like EODT and R45M, had cis, trans, and vinyl C=C groups. In addition, the compound had to be a species for which the EODT mechanism either had an existing (sub)network for decomposing the parent or could readily be expanded to include one. DTE and

MYR met these criteria. The two compounds are liquids at 298 K and 1 atm. Their normal boiling points are approximately 440 K. Products produced by DTE's pyrolysis following heating at temperatures from 450 to 1300 K have been quantified and reported (Pesce-Rodriguez et al. 2023).

As for this mechanism's use for NN training and validation, we plan to employ results produced by it when coupled to models for simulating the compounds' condensed-phase pyrolysis and their combustion in opposed-flow diffusion flame (OPDF) experiments. The compounds' condensed-phase pyrolysis will be simulated with a theorized framework we have proposed and have been investigating for that purpose (Veals et al. 2018; McQuaid et al. 2020). Predicated on free volume theory (Cohen and Turnbull 1959), it includes a function [P_{HFV}] for converting rate coefficients for elementary gas-phase reactions into rate coefficients for elementary condensed-phase reactions. As outlined by us previously (McQuaid et al. 2020), for neat liquids P_{HFV} is parameterizable on the basis of the temperature (T) dependence of their self-diffusion coefficients (D). The effort summarized herein was undertaken in anticipation of the need to parameterize P_{HFV} for DTE and MYR.

As for the model for simulating OPDF experiments, when coupled with condensed-phase density [$\rho(T)$] and enthalpy-of-formation [$\Delta_f H_c(T)$] estimates, it can produce predictions for linear regression rates (McQuaid 2020). Estimates for ρ are a common/standard output of molecular dynamics (MD) simulations. To obtain $\Delta_f H_c(T)$ estimates, we recorded cohesive energies [$E_{coh}(T)$], converted them to enthalpy-of-vaporization [$\Delta H_v(T)$] estimates, and subtracted those estimates from gas-phase enthalpy-of-formation [$\Delta_f H_g(T)$] estimates derived from results produced by quantum mechanics–based electronic structure methods (QM-ESMs).

In addition, we employed Joback group contribution methods (Joback and Reid 1987) to obtain $\rho(T)$, $\Delta H_v(T)$, and $D(T)$ estimates for the two compounds. Reasonable agreement between those estimates and estimates derived from the MD simulations was observed. Requiring considerably less effort to implement than MD-based methods, they appear to warrant consideration for parameterizing models for other pure-component hydrocarbon systems comprising molecules with sizes comparable to DTE and MYR.

2. Computational Methods

The MD protocol employed for this study was similar to that employed for a previous investigation of hydroxyl-terminated oligomers of EODT [HO-(EODT)$_n$-OH] (Veals et al. 2023). The MD simulations were performed with LAMMPS (Plimpton 1995) using the Class-II type COMPASS and PCFF force fields. PCFF

was originally developed to study common organic polymers (Sun 1994). COMPASS (Sun 1998) is effectively an extension of PCFF that includes atom types whose potential parameters have been optimized to produce reliable predictions for the relatively unique electronic and structural properties of energetic functional groups (Bunte and Sun 2000; McQuaid et al. 2003). Although COMPASS was thought to be unnecessary for this study, given the likelihood that it will be employed for future studies of EMs, we were interested in how it would perform. As will be discussed, it produced results that were in better agreement with the validating data we were able to assemble, suggesting COMPASS might be preferable to PCFF for future studies.

2.1 Simulation Setup and Protocols

Figure 1 presents an overview of the methods and protocols employed for this study. The Enhanced Monte Carlo (EMC) tool (in 't Veld and Rutledge 2003) was employed to create and pack molecules into cells. It employed a Monte Carlo algorithm to build the molecules. The molecules' structures are shown in Fig. 2. The assignment of atom types was straightforward. The PCFF force field as implemented in EMC was the basis for generating intramolecular bond lengths and angles. To mitigate any excessively repulsive atom–atom interactions that the EMC-generated configurations might have had, an energy minimization followed by a short constant number, constant pressure, constant temperature (NPT) simulation was performed to reduce them.

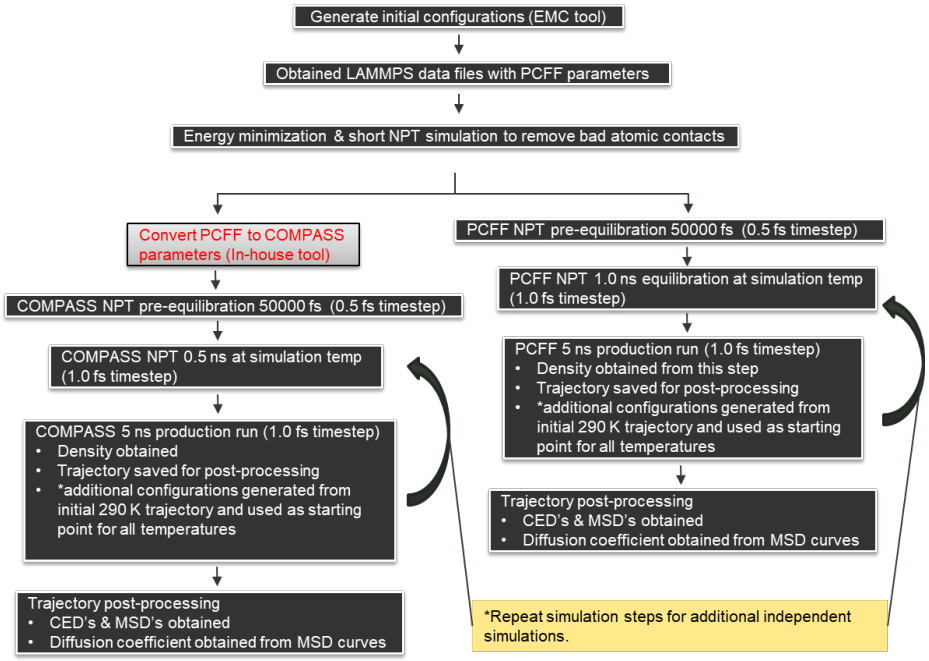

Fig. 1 MD methods and protocols employed to obtain estimates for properties of interest

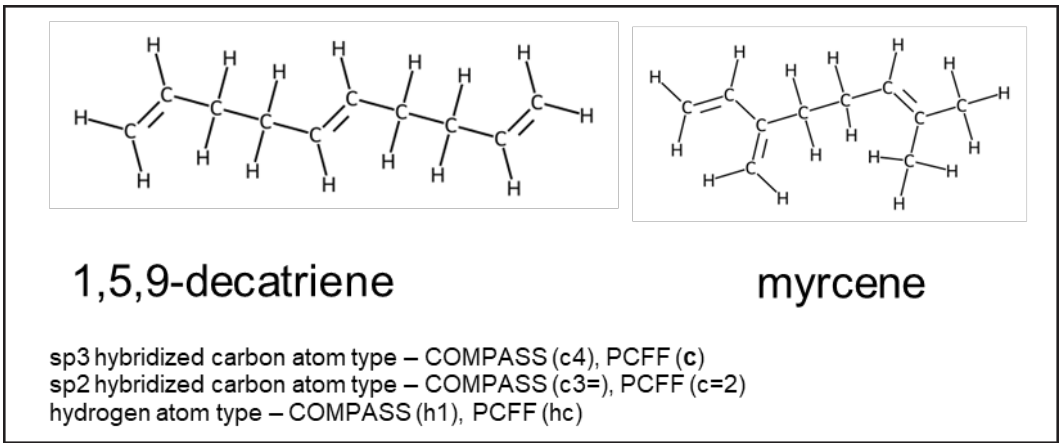

Fig. 2 The molecular structures of 1,5,9-decatriene and myrcene and atom-type assignments for the COMPASS and PCFF force fields

To assess system-size effects on the estimates for $\rho(T)$, $\Delta H_v(T)$, and $D(T)$, simulations were conducted with four different cell sizes: 1,300 atoms (50 molecules), 2,496 atoms (96 molecules), 4,992 atoms (192 molecules), or 10,010 atoms (385 molecules). As shown in the appendix, in each case similar estimates were generated by the systems with 2,496, 4,492, and 10,010 atoms, suggesting the 10,010-atom systems were sufficiently large. The results from the 10,010-atom systems are presented herein.

From the pre-equilibrated cells, the atomic coordinates, atom types, and topology information (i.e., the atomic connectivity patterns and associated coefficients for all force-field potential energy terms) produced with the PCFF-based model were used to create starting configurations for the COMPASS-based model. Because the COMPASS force field is designed for use with Materials Studio modules, to ensure that the force-field parameter conversions were valid, various LAMMPS-generated energy components, including total potential energy, bond energy, angle energy, and torsion energy, were compared to analogous energy components generated using the Forcite module within Materials Studio.

Prior to performing production runs, the pre-equilibrated EMC-generated cells were fully equilibrated via a sequence of three simulations. For these simulations (and the production runs), electrostatic interactions were calculated via an Ewald summation using the particle–particle particle–mesh method implemented in LAMMPS. Short-range van der Waals interactions within a 12.5-Å cutoff limit were calculated with 9-6 Lennard-Jones functions. Pressure was maintained at 1.01325 bar (1 atm) with a Nosé-Hoover barostat. Temperature was maintained at targeted temperatures with a Nosé-Hoover thermostat. The first simulation was a 50-ps NPT run at the target temperature. The second was a 1.0-ns run with the temperature held fixed at the target temperature. Time steps were 1.0 fs. The

preproduction-run equilibration protocol was followed by a 5-ns NPT production run with 1-fs time steps. Relaxation times were 0.1 ps for the thermostat and 1.0 ps for the barostat. Coordinates were saved every 10 ps.

To create additional unique/independent trajectories, 10 arbitrary frames were taken from the production run produced with the first cell, and they were processed via the equilibration protocol prior to performing a production run with them. Subsequent production runs were performed at 250, 273, 290, 298, 350, 400, 450, and 500 K. (The initial configurations for each were from 290-K simulations.) The upper end of the temperature range of interest was established in recognition of the fact that "the rate of evaporation from the free surface of a superheated liquid is extremely great, and superheating of it is practically impossible" (Zeldovich 1942). DTE and MYR have normal boiling points near 440 K. Thus, it was considered likely that results produced at higher temperatures would have little to no value.

2.2 Self-diffusion Coefficients

As discussed by (Maginn et al. 2019), one of the two commonly employed theoretical bases for deriving *D* estimates from MD simulations is the "Einstein" equation, viz.

$$D = \frac{1}{2d_\alpha N} \lim_{t \to \infty} \frac{\langle |\boldsymbol{r}(t) - \boldsymbol{r}(0)|^2 \rangle}{\mathrm{d}t} \quad (1)$$

where d_α is the number of dimensions, *N* is the number of particles, $\langle |\boldsymbol{r}(t) - \boldsymbol{r}(0)|^2 \rangle$ is the mean square displacement (MSD) of the particles' positions $[\boldsymbol{r}(t)]$ at a given time (t) compared to their starting positions $\boldsymbol{r}(0)$. Because Eq. 1 predicates computing *D* values on the basis of MSDs in the limit "$t \to \infty$", prior to a study of HO-(EODT)$_n$-OH oligomers (Veals et al. 2023), we assumed that estimates would improve with an increase in simulation duration. However, Maginn et al. (2019) recommended that they be calculated on the basis of results produced in the "diffusive regime," and that such regimes correspond to a "middle" temporal interval in the simulations. That being said, they were unaware of any objective approach to defining such an interval, stating only that the relationship between MSD and *t* should be approximately linear, and therefore would be characterized by ln(MSD) versus ln(*t*) plots that had a slope approximately equal to 1.

Offering no objective guidance as to how long the simulations needed to be—only that they be long enough to include a region in which the slopes of ln(MSD) versus ln(*t*) plots were approximately equal to 1—we ran simulations of varying durations (t_d) to establish values for which MSD(*t*) plots for $0.25t_d \leq t \leq 0.50t_d$ ($t_0 \leq t \leq t_{max}$) were reasonably well-fit to a linear function. With d_α= 3,

$$D = \frac{m}{6N}, \quad (2)$$

where m is the slope of the MSD(t) plot.

2.3 Thermodynamic Parameters

To obtain $\Delta_f H_c(T)$ estimates for the systems, we subtracted MD-based $\Delta H_v(T)$ estimates from QM-ESM-based $\Delta_f H_g(T)$ estimates. The $\Delta H_v(T)$ estimates were derived from MD-generated cohesive energies (E_{coh}). Defined as the average intermolecular nonbond energy per mole, E_{coh} is related to a material's ΔH_v per

$$\Delta H_v(T) \approx E_{coh}(T) + RT \quad (3)$$

where R is the universal gas constant. The $\Delta_f H_g(T)$ estimates were calculated using the QM-ESM-based thermodynamic property formulae prescribed for them in the EODT mechanism.

3. Results and Discussion

3.1 Density Estimates

Table 1 presents MD-based $\rho(T)$ estimates for DTE and MYR at temperatures from 250 to 500 K. Figure 3 presents the data graphically. As found previously for HO-(EODT)$_n$-OH systems (Veals et al. 2023), COMPASS-based estimates were somewhat higher than PCFF-based estimates, and they were in better agreement with the limited number of measured values we were able to find.

Table 1 COMPASS- and PCFF-based $\rho(T)$ estimates for 1,5,9-decatriene and myrcene

T (K)	1,5,9-decatriene ρ (g/cm^3)			myrcene ρ (g/cm^3)		
	COMPASS	PCFF	Measured	COMPASS	PCFF	Measured
250.15	0.80	0.74		0.82	0.77	
273.15	0.79	0.72		0.80	0.74	
290.15	0.77	0.70		0.79	0.73	
298.15	0.76	0.70	0.765	0.78	0.72	0.795
300.15	0.76	0.69		0.78	0.72	
350.15	0.72	0.65		0.74	0.67	
400.15	0.67	0.60		0.70	0.62	
450.15	0.63	0.54		0.65	0.57	
500.15	0.58	0.48		0.61	0.51	

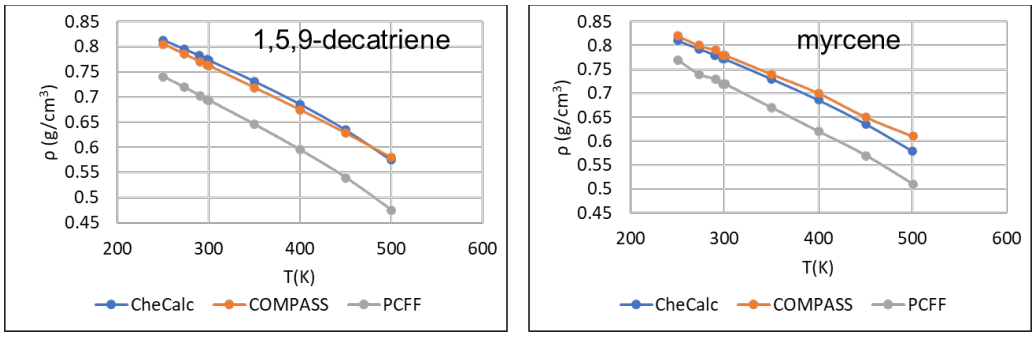

Fig. 3 COMPASS- and PCFF-based $\rho(T)$ estimates for 1,5,9-decatriene and myrcene

As another basis for checking the validity of the MD-based estimates, we obtained estimates using the Joback group contribution method implemented by the CheCalc program (https://checalc.com/solved/property_joback.html). As shown in Fig. 3, the estimates produced by this method were in excellent agreement with the estimates produced via the COMPASS-based simulations. Therefore, for pure-component hydrocarbon systems comparable to DTE and MYR, this method appears to offer an inexpensive and reliable means for obtaining $\rho(T)$ estimates.

3.2 Enthalpy-of-Vaporization Estimates

Table 2 presents MD-based $\Delta H_v(T)$ estimates for DTE and MYR at temperatures from 250 to 500 K. Figure 4 presents this data graphically. As found previously for HO-(EODT)$_n$-OH systems (Veals et al. 2023), COMPASS-based $\Delta H_v(T)$ estimates were somewhat higher than their PCFF-based counterparts, and they were in better agreement with the limited number of measured values we were able to find in the open literature. They were also in better agreement with $\Delta H_v(T)$ values we derived for MYR based on vapor pressures measured at temperatures from 288 to 445 K (Stull 1947).

Table 2 COMPASS- and PCFF-based $\Delta H_v(T)$ estimates for 1,5,9-decatriene and myrcene

T (K)	1,5,9-decatriene ΔH_v (kJ/mol)			myrcene ΔH_v (kJ/mol)			
	COMPASS	PCFF	Measured	COMPASS	PCFF	Measured	Derived[e]
250.15	52.6	43.5		53.3	44.1		
273.15	50.8	41.8		51.5	42.4		
290.15	49.5	40.5		50.2	41.2		47.1
298.15	48.9	39.9	[51.5][a]	49.6	40.7	50.6[b]	46.9
300.15	48.7	39.7		49.5	40.5	45.7[c], 47.0[d]	46.7
350.15	45.0	36.3		46.0	37.2		44.8
400.15	41.6	33.0		42.7	34.0		43.4
450.15	38.2	29.6		39.4	30.9		
500.15	35.0	26.2		36.3	27.6		

[a] Value for *n*-decane (Viton et al. 1998). [b] van Roon et al. (2002). [c] At 302 K (Stephenson and Malanowski 1987). [d] At 318 K (Bukala et al. 1954). [e] Based on fitting the Clausius-Clapeyron equation to an expression for myrcene's vapor pressure derived from data reported by Stull (1947).

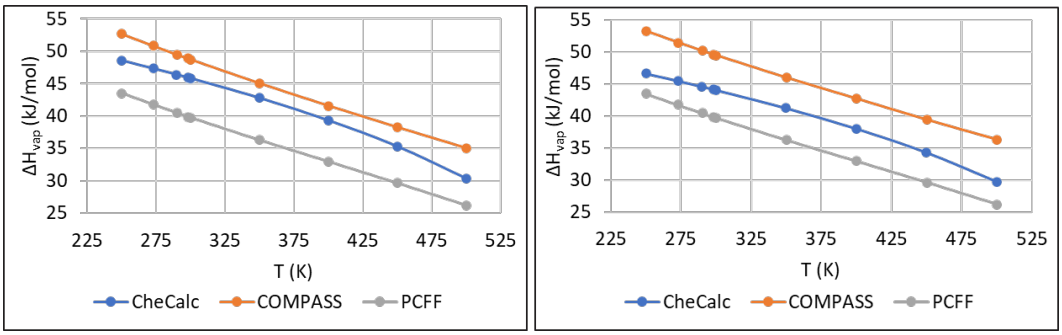

Fig. 4 $\Delta H_v(T)$ estimates for 1,5,9-decatriene and myrcene

As another basis for checking the validity of the MD-based estimates, we obtained estimates using the CheCalc implementation of the Joback group contribution method. As shown in Fig. 4, the estimates produced by this method fell between the estimates produced via the COMPASS-based and PCFF-based MD simulations. Therefore, for pure-component systems comparable to DTE and MYR, this method appears to offer an inexpensive, reasonably reliable alternative for obtaining $\Delta H_v(T)$ estimates.

3.3 Condensed-Phase Enthalpy-of-Formation Estimates

We found the QM-ESM-based $\Delta_f H_g(T)$ estimates (in kJ/mol) for DTE at temperatures from 250 to 500 K were well-represented by the formula

$$\Delta_f H_g^{DTE}(T) = 76.25 + 5.784\text{x}10^{-2}T + 2.413x10^{-4}T^2 \quad (4)$$

and COMPASS-based $\Delta H_v(T)$ estimates for it (in kJ/mol) were well-represented by the formula

$$\Delta_f H_v^{DTE}(T) = 74.37 - 9.547\text{x}10^{-2}T + 3.357x10^{-5}T^2. \quad (5)$$

Subtracting Eq. 5 from Eq. 4 yields

$$\Delta_f H_c^{DTE}(T) = 1.88 + 1.53\text{x}10^{-1}T + 2.08x10^{-4}T^2. \quad (6)$$

At 298 K, this formula yields 65.9 kJ/mol, which seemed reasonable.

We found the QM-ESM-based $\Delta_f H_g(T)$ estimates (in kJ/mol) for MYR at temperatures from 250 to 500 K were well-represented by the formula

$$\Delta_f H_g^{MYR}(T) = 39.04 + 3.961\text{x}10^{-2}T + 2.605\text{x}10^{-4}T^2 \quad (7)$$

and COMPASS-based $\Delta H_v(T)$ estimates for it (in kJ/mol) were well-represented by the formula

$$\Delta_f H_v^{MYR}(T) = 74.01 - 9.092\text{x}10^{-2}T + 3.115\text{x}10^{-5}T^2. \quad (8)$$

Subtracting Eq. 8 from Eq. 7 yields

$$\Delta_f H_c^{MYR}(T) = -34.97 + 1.31\text{x}10^{-1}T + 2.29\text{x}10^{-4}T^2. \quad (9)$$

At 298 K, this formula yields 24.4 kJ/mol. It is approximately 10 kJ/mol higher than a value Cox and Pilcher (1970) derived from an enthalpy-of-combustion measurement for the substance that was reported by Hawkins and Eriksen (1954). This agreement was considered reasonable.

3.4 Self-diffusion Coefficient Estimates

Figure 5 shows independent MSD(t) trajectories for DTE at 250 and 500 K. (The trajectories for MYR were similar.) The simulations were run for 5 ns, and MSD(t) values in the range 1.25 ns < t < 2.50 ns were employed as the basis for computing D. The plots show the variability between simulations, particularly at longer observation times. The MSD(5 ns) values realized in the COMPASS-based simulations were significantly less than those realized in their PCFF-based counterparts. Given the higher $\rho(T)$ estimates produced with COMPASS, lesser MSD(5 ns) values were to be expected.

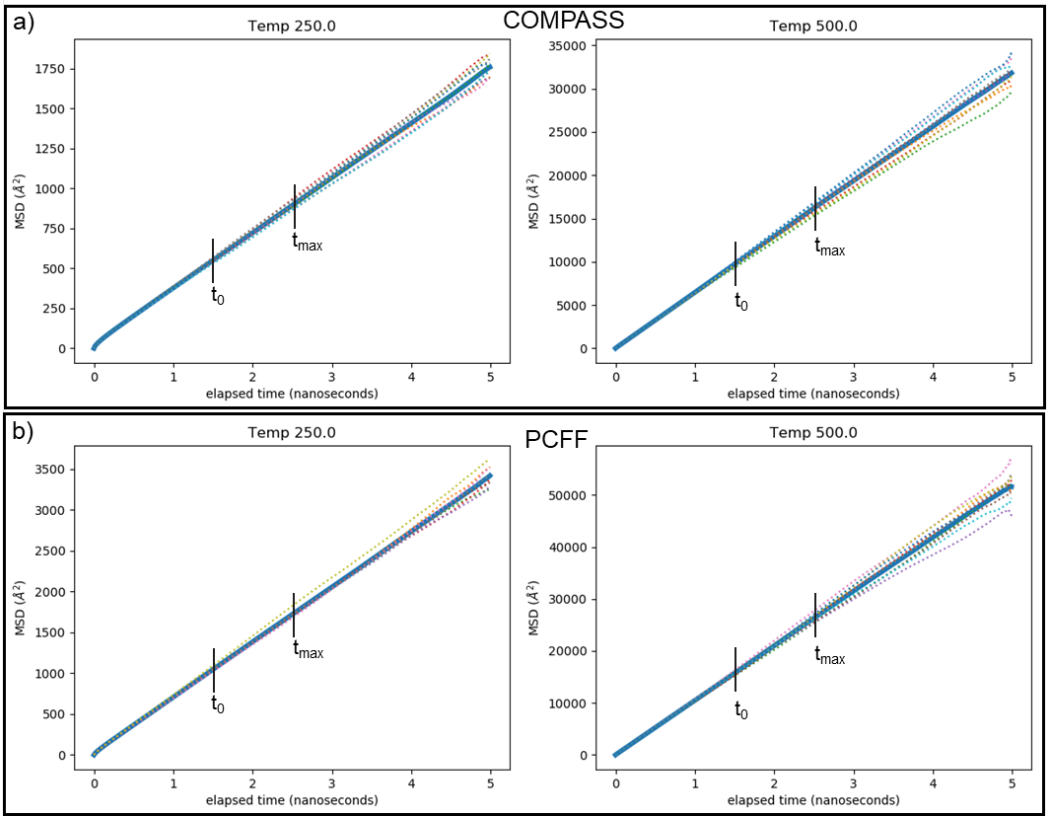

Fig. 5 COMPASS- and PCFF-based MSD versus t trajectories for 1,5,9-decatriene at 250 and 500 K

Tables 3 and 4 present [MSD(5 ns)]$^{1/2}$, $D(T)$, and ln[D(cm^2/s)] estimates for DTE and MYR, respectively. [MSD(5 ns)]$^{1/2}$ values indicate how far 'c3=' (COMPASS) and 'c=2' (PCFF) atom types traveled during the simulations. The values indicated that the 5-ns durations of the simulations were sufficient to produce good $D(T)$ estimates over the entire temperature range of interest.

Table 3 COMPASS- and PCFF-based [MSD(5 ns)]$^{1/2}$, D, and ln(D) estimates for 1,5,9-decatriene

Force field	T	[MSD(5 ns)]$^{1/2}$	D		ln(D)
	K	Å	cm^2/s		
COMPASS	250	42.6	5.91E-06	4.14E-06 [a]	–12.04
	273	53.7	9.51E-06	7.62E-06 [a]	–11.56
	290	62.4	1.29E-05	1.12E-05 [a]	–11.26
	298	67.0	1.47E-05	1.32E-05 [a]	–11.13
	300	68.0	1.54E-05	1.38E-05 [a]	–11.08
	350	92.8	2.87E-05	3.25E-05 [a]	–10.46
	400	118.7	4.73E-05	6.17E-05 [a]	–9.96
	450	147.6	7.38E-05	1.02E-04 [a]	–9.51
	481			7.60E-04 [b]	
	500	178.3	1.08E-04	1.52E-04 [a]	–9.13
PCFF	250	58.9	1.13E-05		–11.39
	273	71.8	1.74E-05		–10.96
	290	82.4	2.25E-05		–10.70
	298	86.9	2.50E-05		–10.60
	300	89.1	2.66E-05		–10.54
	350	116.3	4.60E-05		–9.99
	400	148.3	7.36E-05		–9.52
	450	185.2	1.13E-04		–9.09
	500	227.1	1.76E-04		–8.64

[a] Value for *n*-decane based on graphical data published by Douglass and McCall (1958).
[b] Measured value for *n*-decane published by Bachl and Ludemann (1986).

Table 4 COMPASS- and PCFF-based [MSD(5 ns)]$^{1/2}$, D, and ln(D) estimates for myrcene

Force field	T	[MSD(5 ns)]$^{1/2}$	D	ln(D)
	K	Å	(cm^2/s)	
COMPASS	250.15	40.6	5.57E-06	–12.1
	273.15	51.5	8.71E-06	–11.7
	290.15	60.1	1.20E-05	–11.3
	298.15	64.0	1.34E-05	–11.2
	300.15	64.9	1.40E-05	–11.2
	350.15	88.2	2.59E-05	–10.6
	400.15	113.3	4.34E-05	–10.0
	450.15	141.1	6.63E-05	–9.6
	500.15	169.7	9.52E-05	–9.3
PCFF	250.15	55.3	1.03E-05	–11.5
	273.15	67.1	1.51E-05	–11.1
	290.15	76.2	1.93E-05	–10.9
	298.15	81.4	2.24E-05	–10.7
	300.15	82.7	2.28E-05	–10.7
	350.15	109.6	4.02E-05	–10.1
	400.15	140.6	6.61E-05	–9.6
	450.15	173.5	1.01E-04	–9.2
	500.15	210.5	1.51E-04	–8.8

Attempting to validate these estimates, we searched the open literature for comparable measurement-based results. Values reported for *n*-decane ($C_{10}H_{22}$) were the only ones we could find that appeared to be relevant. Values derived from graphical data published by Douglass and McCall (1958) for temperatures from 250 to 360 K, which we found were well-represented by

$$D(T) = 5.563\text{x}10^{-3}\exp(-1801/T), \tag{10}$$

where D is in squared centimeters per second and T is in kelvin, are compared to the COMPASS-based D estimates in Table 3. These data were in reasonable agreement with the MD-based estimates. However, Bachl and Ludemann (1986) reported a measurement-based D value for *n*-decane at 481 K (7.6×10^{-4} cm^2/s) that was considerably higher than would be inferred from the other two sets.

Given the limited number of relevant measurement-based $D(T)$ values, we hoped we might be able to couple measurement-based viscosities (η) and established relationships between η and D to obtain another basis for validating the MD-based D estimates. However, the only measured η values that we found that we trusted to be (somewhat) relevant were for *n*-decane. And even that data was limited.

The search did, however, identify the potential to obtain estimates via the CheCalc implementation of the Joback group contribution method. Results it produced for DTE are presented in Table 5. (Results for MYR were not directly obtainable because there were no coefficients for its =C< groups.)

Following Dullien's (1972) approach for relating $\eta(T)$ and $D(T)$, viz.

$$D(T) = \frac{RT\left(\frac{d}{2.2}\right)^2 MW}{\rho(T)\eta(T)} \tag{11}$$

setting d equal to Dullien's value for n-decane (6.62 Å) and using the COMPASS-based $\rho(T)$ estimates, we converted the $\eta(T)$ estimates into $D(T)$ estimates. Shown in Table 5, they are compared to the COMPASS- and PCFF-based $D(T)$ estimates in Fig. 6. Falling between the COMPASS- and PCFF-based $D(T)$ estimates, the CheCalc-based $D(T)$ estimates increased our confidence in the MD-based estimates. Moreover, the comparison strongly suggested that the CheCalc-based estimates, which are trivial to compute, could be employed to parameterize models for other pure-component hydrocarbon systems that we can imagine might be desirable for NN training and validation.

Table 5 CheCalc-based $\eta(T)$ and $D(T)$ estimates for 1,5,9-decatriene

T (K)	η (cP)	D(cm^2/s)
250.15	1.19	9.35E-06
273.15	0.82	1.46E-05
290.15	0.65	1.91E-05
298.15	0.58	2.15E-05
300.15	0.57	2.22E-05
350.15	0.34	4.13E-05
400.15	0.23	6.50E-05
450.15	0.17	9.32E-05
500.15	0.13	1.22E-04

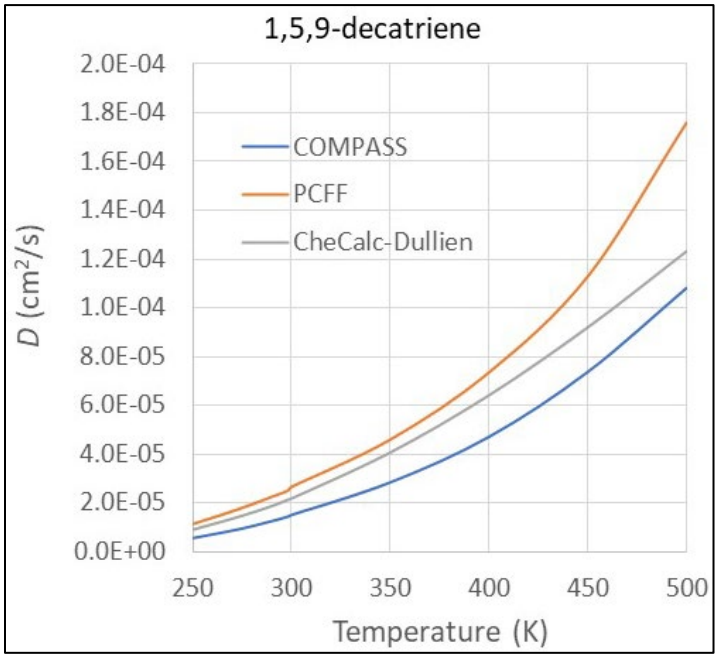

Fig. 6 $D(T)$ estimates for 1,5,9-decatriene

Curious about the method's inability to produce estimates for MYR, we investigated the matter. In the Joback method, $\eta(T)$ is estimated per

$$\eta(T) = MW * \exp\left(\frac{A}{T} + B\right) \tag{12}$$

where

$$A = -597.82 + \sum_i n_i a_i, \tag{13}$$

$$B = -11.202 + \sum_i n_i b_i, \tag{14}$$

n_i is the number of groups (i) in the molecule, and the parameters a_i and b_i are constants that have been established for each group. The method did not produce estimates for MYR because it lacked a_i and b_i for =C< groups.

Given the method's capacity to yield $D(T)$ estimates for DTE that agreed with the MD-based $D(T)$ estimates, we wondered whether the COMPASS- and PCFF-based $D(T)$ estimates for MYR could be employed to establish $a_{=\mathrm{C}<}$ and $b_{=\mathrm{C}<}$. Therefore, we converted the MD-based $D(T)$ estimates into $\eta(T)$ estimates via Eq. 11, then by trial and error established $a_{=\mathrm{C}<}$ and $b_{=\mathrm{C}<}$ values that would, in conjunction with the a_i and b_i established for MYR's other groups, split the difference between the COMPASS- and PCFF-based $\eta(T)$ estimates. The results produced with $a_{=\mathrm{C}<}$ = -310 and $b_{=\mathrm{C}<}$ = 1.2 are compared to the MD-based $\eta(T)$ estimates in Fig. 7. These coefficients are very similar to the coefficients established for >CH- groups: $a_{>\mathrm{CH}-}$ = –322.15 and $b_{>\mathrm{CH}-}$ = 1.187. Thus, we believe they warrant use if needed.

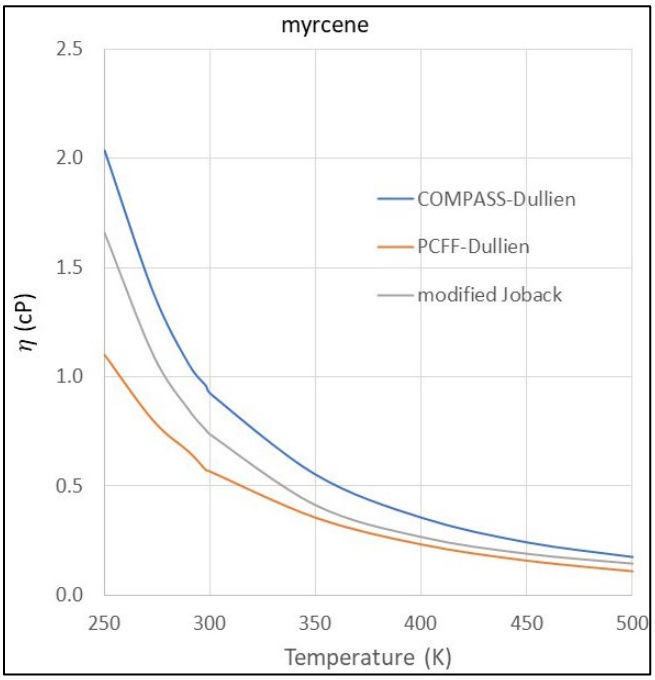

Fig. 7 Comparison of $\eta(T)$ predictions for myrcene

3.5 Probability Function Parameterizations

As discussed in a previous publication (McQuaid et al. 2020), we have proposed and investigated a framework for estimating rate coefficients for elementary condensed-phase reactions that includes a function $[P_{HFV}]$ for computing the probability that potential reactive sites are proximate to a free volume hole that is large enough for a reaction to proceed unhindered, and prevented from reversing by a concomitant diffusive jump "behind" it. Predicated on free volume theory, $P_{HFV}(T)$ is related to $D(T)$ per

$$D(T) = AP_{HFV}(T) = A\exp\left(\frac{-B}{T-T_0}\right) \tag{15}$$

where A, B, and T_0 are temperature-independent constants derivable by fitting Eq. 15 to $D(T)$ estimates.

Figure 8 shows the COMPASS- and PCFF-based $\ln[D(T)]$ estimates for DTE and MYR and fits of $\ln(A) - [B/(T - T_0)]$ to the data. As found for liquid nitrate esters (McQuaid et al. 2020), $\exp(-B/(T - T_0))$ appeared to reasonably represent the temperature-dependence of D. The values for B and T_0 derived from the $D(T)$ estimates produced by the COMPASS and PCFF force fields were considerably different. However, with respect to computing $P_{HFV}(T)$, the pairs' values were offsetting to a degree; the smaller B/numerator produced by the COMPASS-based $D(T)$ estimates coupled with a smaller denominator because $|-T_0|$ was smaller. Compared to T_0 values published by Zielinski and Duda (1992) for other hydrocarbons, neither T_0 appears to be physically unrealistic. The COMPASS-based T_0 values (i.e., –47.8 K for DTE and –29.9 K for MYR) were in better agreement with the T_0 value Zielinski and Duda (1992) reported for *n*-octane (–37.4 K). Thus, we suspect they will be found to be in better agreement with the actual value than the PCFF-based values.

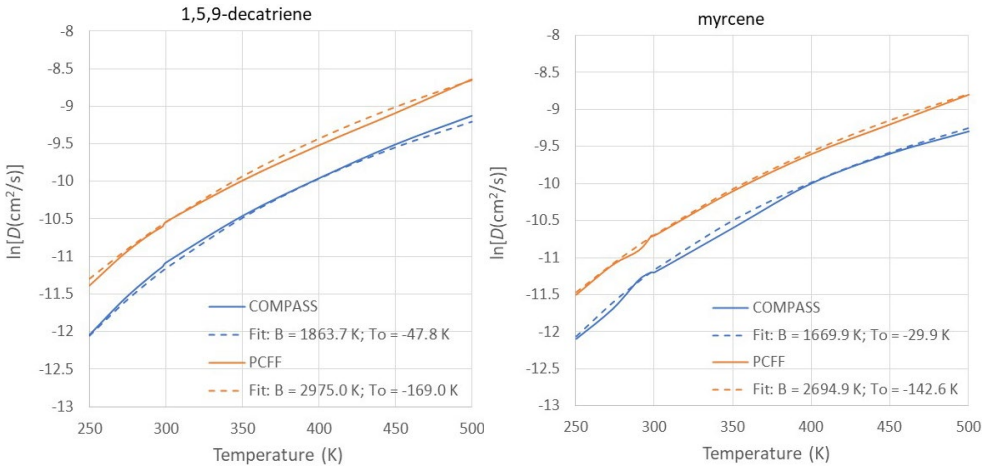

Fig. 8 ln[$D(T)$] estimates for 1,5,9-decatriene and myrcene and fits of Eq. 15 to the data

Figure 9 shows the $P_{HFV}(T)$ values produced by the parameterizations. Per our theorized framework, they predict that at 300 K, condensed-phase rate coefficients will be less than 1% of their gas-phase counterparts. And at 500 K, condensed-phase rate coefficients will be less than 5% of their gas-phase counterparts. The validity of these predictions remains to be corroborated.

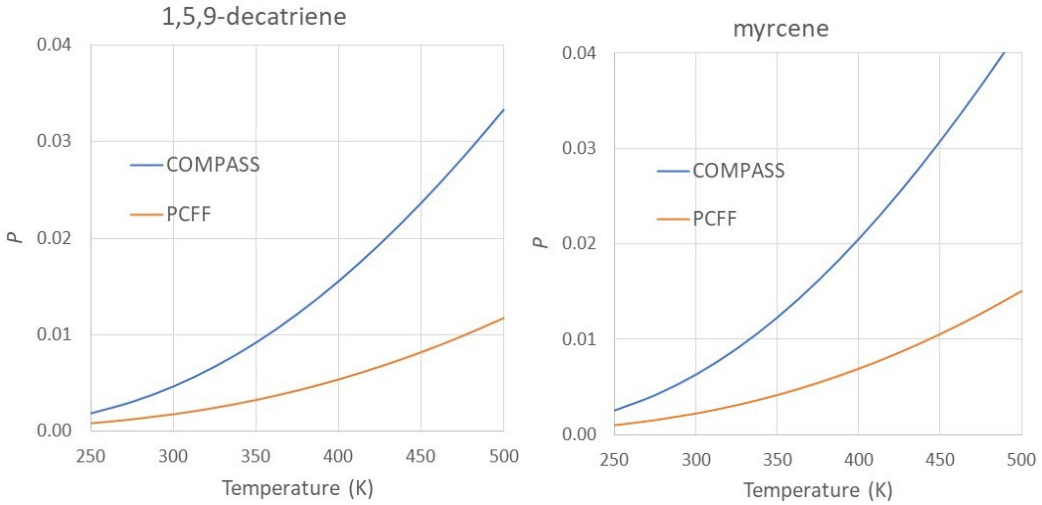

Fig. 9 $P_{HFV}(T)$ **estimates for 1,5,9-decatriene and myrcene**

4. Conclusion

In support of a program to develop and apply ML methods to accelerate the creation of detailed finite-rate chemical kinetics mechanisms, MD methods were employed to obtain $\rho(T)$, $\Delta H_v(T)$, and $D(T)$ estimates for condensed-phase DTE and MYR. Comparisons with the limited number of relevant measurement-based values we were able to find suggest their merit. COMPASS-based estimates were in better agreement with measurement-based values than PCFF-based estimates. We also found that estimates for these three properties that were produced by CheCalc implementations of Joback group contribution methods were in reasonable agreement with the MD-based estimates. Being significantly cheaper than MD-based methods, such estimates could prove valuable for parameterizing models for other pure-component hydrocarbon systems that can be employed for NN training and validation. Group contribution coefficients to employ for estimating $\eta(T)$ values for pure-component hydrocarbon systems with >C= groups were obtained and may find application as well.

We also combined $\Delta H_v(T)$ estimates with $\Delta_f H_g(T)$ estimates based on QM-ESMs to obtain $\Delta_f H_c(T)$ estimates for DTE and MYR. They appeared reasonable. In addition, the $D(T)$ estimates were employed to parameterize $P_{HFV}(T)$. Those results indicate that at temperatures up to 500 K, the rate coefficients for elementary

condensed-phase reactions will be less than 5% of their gas-phase counterparts. That prediction remains to be corroborated.

5. References

Bachl F, Ludemann H-D. Pressure and temperature dependence of self-diffusion in liquid linear hydrocarbons. Zeitschrift für Naturforschung. 1986;41a:963–970.

Bukala M, Majewski J, Rodzinski W. Przem Chem. 1954;10:6.

Bunte SW, Sun H. Molecular modeling of energetic materials: the parameterization and validation of nitrate esters in the COMPASS force field. J Phys Chem B. 2000;104:2477–2489.

Chen CC, Stone CP, McQuaid MJ, Veals JD. A detailed gas-phase finite-rate chemical kinetic mechanism for modeling the pyrolysis of 1,5,9-decatriene. Proceedings of the 44th JANNAF Propellant and Explosives Development and Characterization Subcommittee Meeting; 2023.

Cohen MH, Turnbull D. Molecular transport in liquids and glasses. J Chem Phys. 1959;31:1164–1169.

Cox JD, Pilcher G. Thermochemistry of organic and organometallic compounds. Academic Press; 1970. p. 1–636.

Douglass DC, McCall DW. Diffusion in paraffin hydrocarbons. J Phys Chem. 1958;62:1102–1107.

Dullien FAL. Predictive equations for self-diffusion in liquids: a different approach. AlChE J. 1972;18:62–70.

Hawkins JE, Eriksen WT. Physical and thermodynamic properties of terpenes. II. The heats of combustion of some terpene hydrocarbons. J Am Chem Soc. 1954;76:2669.

in ‘t Veld PJ, Rutledge GC. Temperature-dependent elasticity of a semicrystalline interphase composed of freely rotating chains. Macromolecules 2003;36(19):7358–65. https://doi.org/10.1021/ma0346658.

Joback KG, Reid RC. Estimation of pure-component properties from group-contributions. Chem Eng Commun. 1987;57:233–243.

Maginn EJ, Messerly RA, Carlson DJ, Roe DR, Elliot JR. Best practices for computing transport properties 1. Self-diffusivity and viscosity from equilibrium molecular dynamics. Living J Comput Mol Sci. 2019;1:6324–6324.

McQuaid MJ. Modeling the combustion of opposed flows of butadiene and air: a skeletal finite-rate chemical kinetics mechanism derived from the San Diego mechanism and regression rate predictions for hydroxyl-terminated polybutadiene-air systems. DEVCOM Army Research Laboratory (US); 2020. Report No.: ARL-TR-8918.

McQuaid MJ, Sun H, Rigby D. Development and validation of COMPASS force field parameters for molecules with aliphatic azide chains. J Comput Chem. 2003;25:61–71. https://doi.org/10.1002/jcc.10316.

McQuaid MJ, Veals JD, Yeh IC, Chen CC. The development of detailed finite-rate chemical kinetics mechanisms for modeling decomposition in condensed phases. Part 2. The parameterization of free volume theory for liquid nitrate esters. Proceedings of the 50th JANNAF Combustion Subcommittee Meeting; 2020.

Pesce-Rodriguez R, Chen CC, McQuaid MJ. Toward validating a framework for modeling high-throughput analytical techniques employed for energetic material screening. Part 1. Desorption/pyrolysis-gas-chromatography/mass spectrometry (D/P-GC/MS) results for 1,5,9-decatriene. DEVCOM Army Research Laboratory (US); 2023. Report No.: ARL-TN-1148.

Plimpton S. Fast parallel algorithms for short-range molecular-dynamics. J Comput Phys. 1995;117:1–19.

Stephenson RM, Malanowski S. Handbook of the thermodynamics of organic compounds. Springer; 1987. https://doi.org/10.1007/978-94-009-3173-2.

Stull DR. Vapor pressure of pure substances. organic and inorganic compounds. Ind Eng Chem. 1947;39:517–540.

Sun H. Force field for computation of conformational energies, structures, and vibrational frequencies of aromatic polyesters. J Comput Chem. 1994;15:752–768.

Sun H. COMPASS: An ab initio force-field optimized for condensed-phase applications - overview with details on alkane and benzene compounds. J Phys Chem B. 1998;102:7338–7364. http://dx.doi.org/10.1021 /jp980939v.

van Roon A, Parsons JR, Govers HAJ. Gas chromatographic determination of vapour pressure and related thermodynamic properties of monoterpenes and biogenically related compounds, J Chrom A. 2002;955(1):105–115. https://doi.org/10.1016/S0021-9673(02)00200-5.

Veals JD, Yeh IC, Chen CC, Andzelm J, McQuaid MJ. Establishing and parameterizing rate coefficient functions for steps in the decomposition of nitrate esters in condensed phases: progress in developing a practical approach. Proceedings of the 41st JANNAF Propellant and Explosives Development and Characterization Subcommittee Meeting; 2018.

Veals JV, Chen CC, Yeh IC, Stone CP, McQuaid MJ, Dennis CN. Property estimates for hydroxyl-terminated polybutadiene (HTPB) type R45M derived from atomistic molecular dynamics simulations. DEVCOM Army Research Laboratory (US); 2023 June. Report No.: ARL-TR-9714.

Viton C, Chavret M, Jose J. Enthalpy of vaporization of n-alkanes (from nonane to pentadecane). experimental results - correlation. In: Caliste JP, Truyol A, Westbrook JH, editors. Thermodynamic modeling and materials data engineering. Data and knowledge in a changing world. Springer; 1998. https://doi.org/10.1007/978-3-642-72207-3_3.

Zeldovich YB. On the theory of combustion of powder and explosives. Zh Eksp Teor Fiz. 1942;12:498–524.

Zielinski JM, Duda JL. Predicting polymer/solvent diffusion coefficients using free-volume theory. AIChE J. 1992;38:405–415.

Appendix. Property Predictions for 1,5,9-Decatriene and Myrcene as a Function of Simulation Cell Size

Property predictions produced by atomistic molecular dynamics (MD) methods can be a function of the number of atoms in the simulation cells until a certain threshold is exceeded. However, lacking any a priori basis for establishing what that threshold is, we computed for 1,5,9-decatriene and myrcene the three properties of interest—densities (ρ), enthalpies of vaporization (ΔH_v), and self-diffusion coefficients (D)—using four different cell sizes: 1,300 atoms (50 molecules), 2,496 atoms (96 molecules), 4,992 atoms (192 molecules), or 10,010 atoms (385 molecules). COMPASS and PCFF force fields were used.

Comparisons of the estimates produced by each force field with the different cell sizes are shown in Figs. A-1 through A-3. They indicated that the threshold needed for the estimates to be reliable was approximately 2496 atoms. Estimates produced with cells comprising 10,010 atoms are reported.

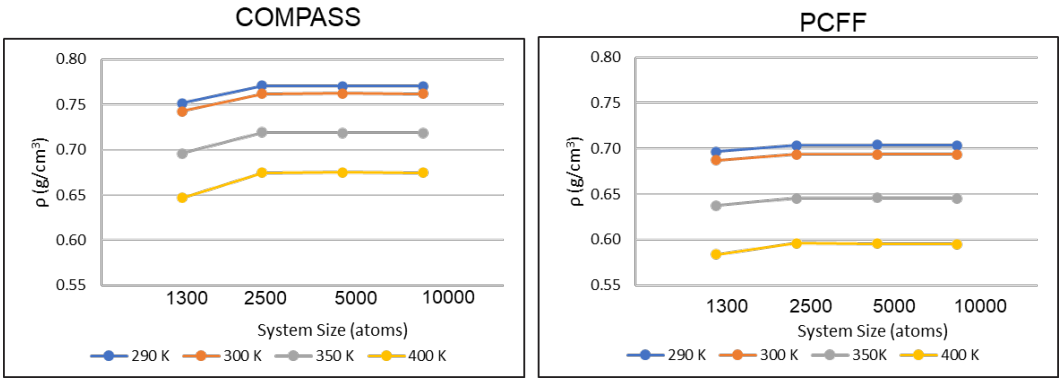

Fig. A-1 COMPASS- and PCFF-based $\rho(T)$ estimates for 1,5,9-decatriene as a function of system size

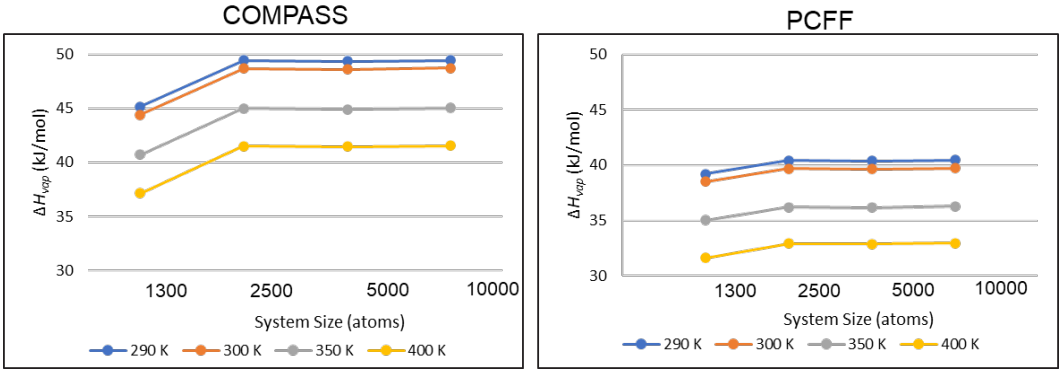

Fig. A-2 COMPASS- and PCFF-based $\Delta H_v(T)$ estimates for 1,5,9-decatriene as a function of system size

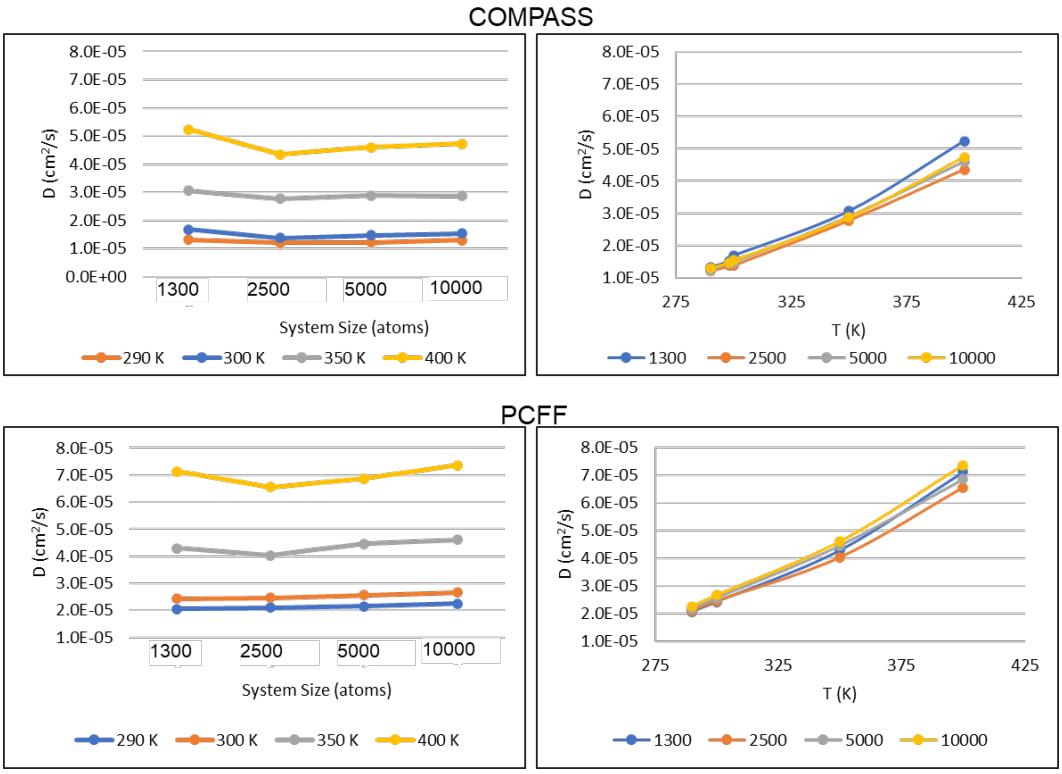

Fig. A-3 COMPASS- and PCFF-based $D(T)$ estimates for 1,5,9-decatriene as a function of system size

List of Symbols, Abbreviations, and Acronyms

ARL	Army Research Laboratory
DEVCOM	US Army Combat Capabilities Development Command
DTE	1,5,9-decatriene
EM	energetic material
EMC	Enhanced Monte Carlo
LAMMPS	Large-scale Atomic/Molecular Massively Parallel Simulator
MD	molecular dynamics
ML	machine learning
MSD	mean square displacement
MYR	myrcene
NN	neural network
NPT	constant number, constant pressure, constant temperature
OPDF	opposed-flow diffusion flame
PCFF	polymer-consistent force-field
QM-ESMs	quantum mechanics-based electronic structure methods

1 (PDF) DEFENSE TECHNICAL INFORMATION CTR
DTIC OCA

1 (PDF) DEVCOM ARL
FCDD RLB CI
TECH LIB

14 (PDF) DEVCOM ARL
FCDD RLA MG
I-C YEH
FCDD RLA WA
N TRIVEDI
E BYRD
B BARNES
R PESCE-RODRIGUEZ
FCDD RLA WC
M MCQUAID
C-C CHEN
C STONE
J VEALS
M MINNICINO
R CORNELL
M NUSCA
FCDD RLD CD
J VEALS
FCDD RLR A
J CIEZAK

1 (PDF) NAWCWD
C DENNIS

1 (PDF) OFFICE NAV RSCH
C STOLTZ

5 (PDF) NAV RSCH LAB
B BOJKO
T LOEGEL
A EPSHTEYN
CJ PFUZNER
IV SCHWEIGERT

3 (PDF) PURDUE UNIV
C GOLDENSTEIN
S SON
T POURPOINT